

Crowd-Resilient Wi-Fi Indoor Localization Framework Using Ensemble Regression Models

N. Bandirmali Erturk , T. Tekkol 

Necla Bandirmali Erturk*

Department of Computer Engineering
Bandirma Onyedi Eylul University, TR
Balikesir, Bandirma, TR

*Corresponding author: nerturk@bandirma.edu.tr

Tugba Tekkol

Department of Computer Engineering
Bandirma Onyedi Eylul University, TR
Balikesir, Bandirma, TR
ttekkol@bandirma.edu.tr

Abstract

This paper presents a machine learning (ML)-based framework to predict performance degradation in Wi-Fi indoor localization systems (ILSs) under varying moving human crowd densities. While indoor localization can be performed in both mobile and fixed wireless settings, the majority of prior research emphasizes mobile devices in motion. In contrast, this study adopts a fixed-wireless configuration, where a smartphone node was held stationary while moving human density varied around it. This design particularly isolates the effect of human crowd-induced interference on received signal strength indicator (RSSI) fluctuations, enabling a controlled evaluation of ML-based error compensation, which is a perspective rarely explored in the literature. Accelerometer-derived motion features were integrated with RSSI measurements, and baseline localization errors were calculated using the conventional Weighted Least Squares (WLS) indoor localization algorithm. Three main ML regression models namely Random Forest, CatBoost, and XGBoost were trained and evaluated. Among them, CatBoost demonstrated the best performance, achieving a root mean squared error (RMSE) of 0.331 m compared to the WLS baseline error of 1.405 m, corresponding to a 76.47% improvement in localization accuracy. The evaluation was intentionally limited to a single indoor layout with a stationary device to isolate crowd-induced RSSI distortions, and multi-position validation and mobile-user scenarios are reserved for future work. The findings confirm that smartphone sensor-fused ML models can anticipate human crowd-induced localization errors and enhance the robustness of multilateration-based ILSs.

Keywords: indoor localization, wireless localization, human crowd, localization error correction, ensemble regression, Wi-Fi, smartphone, accelerometer.

1 Introduction

Indoor localization systems (ILSs) have become essential for enabling location-based services mainly in Global Positioning System (GPS)-denied environments such as shopping malls, airports, hospitals, and industrial facilities. While the GPS provides highly accurate solutions in open outdoor settings, its signal propagation is severely attenuated in enclosed or underground spaces, rendering it unsuitable for indoor environments [35].

Among various indoor localization technologies [17], Wi-Fi-based localization systems are widely adopted due to their compatibility with existing wireless infrastructure and relatively low deployment cost [27]. They typically rely on Received Signal Strength Indicator (RSSI) values for estimating user location through methods such as trilateration, multilateration or fingerprinting. However, RSSI-based localization is highly susceptible to several environmental dynamics, particularly the presence and movement of human crowds, whose mitigation is the main focus of this presented work. Human bodies can absorb and scatter radio signals, inducing multipath effects and signal attenuation that significantly degrade localization accuracy [31].

Traditional trilateration and multilateration Wi-Fi localization techniques typically assume static propagation conditions and do not explicitly account for the spatiotemporal dynamics introduced by varying human crowd densities. Consequently, their performance can degrade significantly in populated indoor environments. Addressing this issue is crucial for maintaining acceptable localization accuracy in real-world scenarios with respect to the emerging mobile and web application services offered by the ever-increasing number of companies [2]. This study introduces a problem-driven methodological reformulation, validates robustness under unseen crowd densities, and provides interpretable insights into crowd-induced signal distortions, rather than proposing yet another indoor localization algorithm.

To address these challenges, recent research has proposed machine learning (ML) approaches that model the complex, non-linear relationships between RSSI values and localization errors, thereby offering improved adaptability and robustness in dynamically changing indoor environments [34], [15]. In particular, ensemble-based ML models have shown promise in learning the underlying patterns of signal degradation under varying human presence.

Furthermore, multi-sensor fusion strategies incorporating inertial measurement units (IMU) have been explored to enhance indoor localization performance beyond what RSSI alone can achieve [18]. These sensor fusion methods are particularly valuable in scenarios where radio signal propagation is highly perturbed by human crowd movement or mobile device dynamics.

Building upon this foundation, we propose a supervised ML framework that integrates RSSI measurements, moving human crowd density levels, and smartphone accelerometer-derived motion features to predict and particularly mitigate human crowd-induced deviations in Wi-Fi indoor localization accuracy. Although the accelerometer data was collected while the device remained stationary, it was included to investigate whether subtle environmental effects such as signal reflections, floor vibrations, or minor device shifts caused by the presence and movement of nearby individuals could be captured through inertial sensing. In this sense, the accelerometer features were not only used to complement RSSI data but also to explore their potential sensitivity to moving human-induced environmental dynamics. The proposed model leverages three ensemble regressors, namely Random Forest, CatBoost, and XGBoost, which were evaluated using both five-fold cross-validation and an independent test dataset to assess their generalization performance.

The contributions of this paper are summarized as follows:

- We conducted a controlled experimental study to analyze the degradation of Wi-Fi-based indoor localization accuracy under varying and moving human crowd densities.
- We formulated crowd-induced RSSI distortion as a learnable disturbance component and proposed a sensor-assisted mitigation framework.
- We collected a comprehensive dataset that includes RSSI measurements and inertial sensor data (accelerometer) across six human density scenarios (0, 4, 8, 12, 16, 20 moving people).

- We developed and evaluated supervised ML models to predict deviations in localization error, offering a data-driven mechanism to estimate the impact of moving human presence on multilateration-based localization. Among the tested models, CatBoost achieved the best performance with a root mean squared error (RMSE) of 0.331 m, compared to the WLS localization baseline error of 1.405 m, corresponding to a 76.47% improvement in localization accuracy.
- We provided extensive validation results using multiple regression metrics to benchmark the generalizability and robustness of the proposed ML framework. CatBoost reached a Coefficient of Determination (R^2) of 0.926, with Mean Absolute Error (MAE) = 0.241 m and Adjusted R^2 = 0.923, demonstrating superior prediction accuracy over Random Forest and XGBoost.

The rest of this paper is organized as follows: Section 2 reviews related work on Wi-Fi-based indoor localization and the effects of moving human crowds on localization accuracy. Section 3 describes the experimental setup and data collection procedures carried out in a controlled indoor environment. Section 4 presents the methodology for feature extraction and error computation. Section 5 introduces the proposed ML framework and explains its implementation details. Section 6 provides evaluation and validation results based on multiple performance metrics to assess model generalizability, followed by discussions about the findings and their broader implications in Section 7. Finally, Section 8 concludes the paper and suggests potential directions for future research and emerging applications.

2 Related Work

ILSs are indispensable in GPS-denied environments such as malls, hospitals, airports, and industrial settings. However, precise indoor localization continues to pose significant challenges due to factors like signal attenuation, multipath effects, and environmental dynamics caused by moving human crowd in addition to the other stationary objects [21]. As key parts of the presented work, fundamentals of the Wi-Fi indoor localization, indoor localization errors induced by human presence and movement, deployment of smartphone IMU sensor fusion for improved localization accuracy, and ML-based approach for crowd-aware indoor Wi-Fi localization are detailed in this section.

2.1 Wi-Fi Indoor Localization

The widespread availability and cost-effectiveness of Wi-Fi infrastructure have made it one of the most preferred technologies in ILS solutions. Wi-Fi-based ILSs utilize various signal measurements to determine the fixed or mobile user's location. Among the most prominent of these are the RSSI, Channel State Information, and Time of Flight (ToF) [6]. Due to its ease of deployment and compatibility with commercially available mobile devices, RSSI has become the most commonly used metric in the literature. RSSI measures the strength of the signal received from access points at the client device, and based on these values, indoor localization techniques such as trilateration, multilateration and fingerprinting are widely applied [37].

However, RSSI signals are highly susceptible to environmental factors, well-studied in the literature. In particular, phenomena such as multipath propagation, signal shadowing, physical obstacles like walls and furniture, hardware discrepancies between devices, and human presence & movement contribute to a high degree of variability in RSSI values, leading to practically poor localization estimations. This variability becomes especially prominent in dynamic environments where human crowd density and especially mobility are high. As a result, RSSI-based indoor localization methods suffer from issues of low accuracy and reliability, which in turn hinders the ability of such systems to meet the demands of real-time and precise indoor localization [4].

2.2 Stationary and Moving Human Crowd Effects on Precise Indoor Localization

ILSs can experience significant performance degradation, particularly in crowded environments. One of the main causes of this decline is the physical and electromagnetic impact that moving human bodies exert on radio signals within indoor spaces. Since the human body is composed largely of salt and water, it tends to absorb a substantial portion of electromagnetic signals, especially at typical

Wi-Fi frequencies such as 2.4 GHz. Furthermore, human presence and movement can scatter the signals by altering their direction of propagation. These effects evidently lead to signal attenuation and distortion before the signal reaches the receiving device of interest [33].

In crowded indoor environments, large numbers of individuals obstruct the direct line-of-sight of wireless radio signals, causing shadowing and intensifying multipath propagation as signals are reflected and scattered through multiple paths. These effects induce significant fluctuations in RSSI measurements, ultimately degrading the performance of localization algorithms [6]. Biswas et al. treated humans not as passive obstacles but as dynamic agents whose body shape and motion alter RSSI characteristics; by applying the mode of RSSI, selecting access points with stronger signals, and averaging over k-nearest neighbors (KNN), they were able to suppress such effects and enhance indoor localization accuracy [7]. Ahmad et al. extended this line of work by conducting experiments with multiple participants surrounding a mobile device, demonstrating that RSSI attenuation grows sharply with human crowd size and proximity, and that the impact is more pronounced under line-of-sight (LOS) than non-line-of-sight (NLOS) conditions [1]. Similarly, Booranawong et al. observed in indoor experiments that human presence and movement significantly increases RSSI variability and localization errors; their application of an aperture thresholding filter reduced error by up to 44% and standard deviation by up to 87% across different methods [8]. Building on these significant findings, Alshami et al. introduced the Adaptive Indoor Positioning System (DIPS) model, which integrates dynamic radio map generation, RSS certainty techniques, and explicit modeling of human presence and movement, achieving 98% floor-level accuracy, 92% room-level accuracy, and reducing point error to 1.2 m with an additional 0.2 m improvement when human crowd effects were explicitly considered [3]. Complementarily, Jiao et al. proposed a deep Convolutional Neural Networks (CNN)-based human detection approach combined with a specific human crowd-RSS attenuation model, showing a 1.53 times increase in signal prediction accuracy and reducing localization error to less than 1.37 m in crowded indoor scenarios [12]. As summarized in Table 1, these studies collectively emphasize that human-induced (both presence and movement) interference is a key challenge for precise Wi-Fi-based indoor localization and that diverse mitigation strategies have been proposed to alleviate its impact.

Table 1: Comparative studies on human crowd and movement-induced indoor Wi-Fi localization errors and mitigation methods.

Work by	Experimental Setup	Key Findings	Mitigation / Method
Biswas et al. [7]	Humans modeled as dynamic agents with RSSI affected by body shape and movement	Demonstrated that humans not only block signals but actively alter RSSI patterns	Improved accuracy using RSSI mode selection, access point selection, and KNN averaging
Ahmad et al. [1]	Experiments with 2–13 individuals around a mobile device under LOS and NLOS conditions	RSSI attenuation increases with crowd size and proximity and is stronger in LOS conditions	Quantified the impact of human crowd-induced RSSI attenuation
Booranawong et al. [8]	Indoor tests with moving humans	Human movement causes significant RSSI fluctuations and localization errors	Aperture thresholding filter reduced localization error by 11–44% and standard deviation by 42–87%
Alshami et al. [3]	Dynamic multi-floor indoor environments considering device heterogeneity and human presence	Achieved 98% floor accuracy, 92% room accuracy, and 1.2 m localization error with further reduction when human effects are modeled	DIPS model integrating dynamic radio maps, RSS certainty, and human effects
Jiao et al. [12]	Crowded indoor scenarios with varying population density	Signal prediction accuracy improved by 1.53 times and localization error reduced below 1.37 m	Smartphone camera-based human detection combined with a crowd-aware RSS attenuation model and trilateration
Proposed method in this paper	Real-world indoor room experiments with controlled crowd densities using Wi-Fi RSSI and smartphone inertial sensor data based on a WLS [32] localization baseline	Crowd-induced dynamics degrade WLS localization accuracy and localization error exhibits learnable patterns related to RSSI, crowd density, and motion	Machine learning-based localization error compensation where localization error is modeled as a regression target to refine WLS estimates without modifying the fingerprinting pipeline

In contrast to prior studies that predominantly emphasize fingerprint representation enhancement, dimensionality reduction, or direct end-to-end location estimation under largely static or implicitly

dynamic indoor conditions, this study explicitly addresses the degradation in localization performance caused by human crowd dynamics. Instead of modifying the fingerprinting pipeline or introducing a new localization algorithm, the proposed method reformulates localization error as a learnable variable and explores the use of machine learning to compensate for WLS-based position estimates across different levels of human density. By explicitly modeling crowd-induced effects as explanatory factors and adopting an error-mitigation perspective rather than direct position prediction, the proposed framework differentiates itself from existing ML-based fingerprinting and localization approaches. This design enables seamless integration with conventional RF localization systems and offers a practical solution for improving localization robustness in realistic, crowded indoor environments.

2.3 Use of Smartphone Inertial Data for Mitigating Indoor Localization Errors

To improve indoor localization accuracy, researchers increasingly fuse smartphone inertial measurements with radio-based signals. These motion cues are independent of the wireless channel and help stabilize estimates by compensating for RSSI variability [18].

Surveying smartphone-based methods, Liu et al. reviewed smartphone-based indoor localization methods, highlighting the limitations of Global Navigation Satellite Systems, inertial sensors, and wireless signals in complex indoor settings and dynamics. They emphasized multi-sensor fusion, combining IMUs, Wi-Fi, Bluetooth, and cameras, as a promising approach to improve accuracy and robustness in indoor localization [16]. Along these lines, Poulouse et al. introduced hybrid indoor localization systems that combine smartphone camera-based methods with IMU sensors to improve localization accuracy. While IMU-only and camera-only systems are prone to issues such as sensor drift, electromagnetic interference, and directional sensitivity, the hybrid approach effectively compensates for these limitations [25]. In another study, Xu et al. proposed a deep learning-based ILS called SeqILS, which leverages human crowd-sourced sequential RSS data together with IMU data during offline training, while using only sequential RSS at online localization. They reported an average indoor localization error of 3.37 m, achieving at least 18.4% improvement over conventional and recent deep-learning methods [36].

2.4 Deploying Machine Learning in Indoor Localization

ML has emerged as a powerful tool in addressing the limitations of traditional radio frequency signal-based indoor localization techniques. ML algorithms can be used to successfully model complex, non-linear relationships between input features such as RSSI values, crowd levels, and environmental conditions to predict localization error or location coordinates [24].

Building on this trend, recent work applies ML to both localization error modeling and especially fingerprint pipeline refinement under varying indoor conditions. Salamah et al. proposed a Principal Component Analysis-based framework for Wi-Fi fingerprinting on Android/IEEE 802.11 WLANs that suppresses feature redundancy and noise; across KNN, Decision Tree, Random Forest, and Support Vector Machines (SVM). Their approach improved accuracy while reducing computation time by up to 70% in static and 33% in dynamic scenarios, supporting real-time use [28]. Singh et al. offered an early, comprehensive survey of ML-driven indoor localization with Wi-Fi RSSI fingerprints, covering fingerprint construction, radio-map building, and learning algorithms. They reported consistent gains over conventional techniques, alongside better scalability for Industry 4.0 and 5G/6G services [30]. Extending this perspective, Roy et al. reviewed state-of-the-art ML methods across Wi-Fi, Bluetooth, and related technologies, highlighting the challenges of signal variability and outlining recent advances and future directions in adaptive deep learning and robust model design for improved indoor localization [26].

3 Experimental Setup for the Development of ML-based Model for Precise Wi-Fi Indoor Localization

This section describes the experimental area, hardware/software stack, data-collection protocol, preprocessing pipeline, baseline and deviation definitions, learning setup, and evaluation methodology

used to analyze how human density and mobility degrade Wi-Fi-based indoor localization and to develop an ML model that precisely predicts and compensates the resulting localization error. In this context, the human crowd-induced error mechanism and the proposed mitigation pipeline are presented as a block diagram in Figure 1.

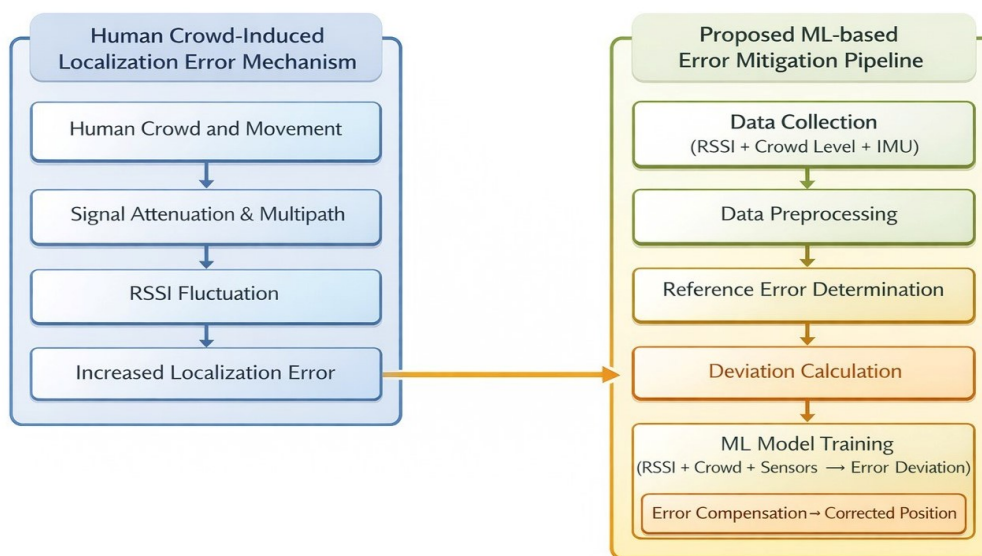


Figure 1: Signal degradation mechanism caused by human crowd and movement, and the proposed ML-based error compensation process.

3.1 Experimental Area

Experiments were conducted in a conference hall measuring 8 m × 16 m with a ceiling height of 4.2 m. Four Wi-Fi access points (APs) were placed at the corners of the rectangular area to maximize spatial coverage, with their coordinates predefined for trilateration-based localization. The fixed smartphone measurement point was located at about the geometric center of the hall, ensuring a consistent line of sight to all APs. In each scenario with varying number of moving human crowd densities, Wi-Fi scans were collected using the custom-developed smartphone mobile application while keeping all other parameters constant. The experimental setup is shown in Figure 2.



Figure 2: Floor plan of the experimental environment with AP and measurement point locations.

3.2 Software, Hardware and Devices

A commercially available Android smartphone was employed as the primary data collection device. The phone was equipped with an IEEE 802.11-compliant Wi-Fi module operating in the 2.4 GHz band

and a MEMS-based tri-axial accelerometer. A custom-developed Android application was installed on the smartphone to simultaneously record RSSI values from the APs and inertial sensor measurements from the accelerometer.

The Wi-Fi APs used in the experiment were standard commercial routers configured to operate solely in beaconing mode without additional traffic. During data collection, no other user devices or personal smartphones were connected to these APs to eliminate interference and ensure that RSSI fluctuations were caused primarily by human presence and movement.

3.3 Data Collection Procedure

RSSI values were collected at a fixed location for moving human density scenarios of 0, 4, 8, 12, 16, and 20 participants. To emulate realistic indoor moving crowd conditions, the participants were instructed to walk casually around the area. As shown in Figure 3, the smartphone remained at about the geometric center of the testbed while walking participants surrounded it, ensuring consistency across all scenarios. This single-position, stationary-device protocol was deliberately selected to control mobility-related confounding factors and to focus specifically on crowd-induced signal dynamics.

For each scenario, approximately 900 valid Wi-Fi scans were obtained over 15 minutes while keeping all other parameters constant. From an initial set of 900 scans per scenario, missing or corrupted samples were removed, resulting in 630 usable data points. Across six scenarios, these processed measurements yielded a total of 3780 samples, which were converted into CSV format and used for model training.

In parallel, three-axis accelerometer data were continuously recorded even though the smartphone remained stationary; these inertial traces were retained to enable future sensor fusion studies and to evaluate their potential for improving ML-based localization accuracy under varying human crowd conditions.

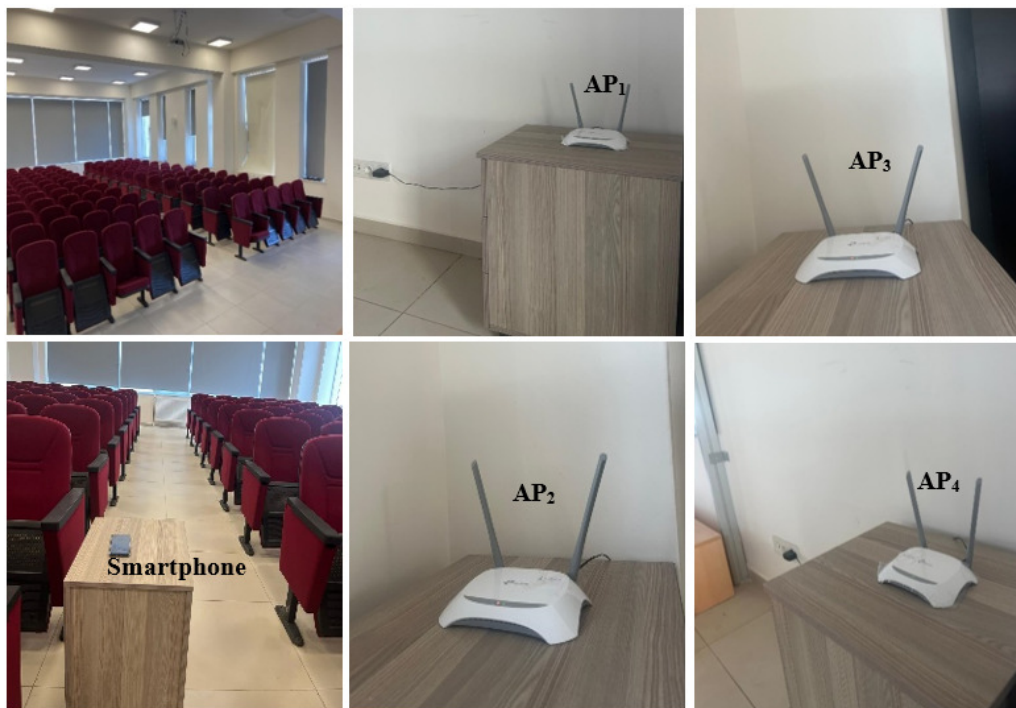


Figure 3: Indoor experimental environment and equipment used for data collection.

4 Methodology

This section explains the procedures for data preprocessing, feature extraction, error calculation, and the modeling strategy used to predict localization degradation in moving human-crowded indoor environments.

4.1 Data Preprocessing

Following data collection, a structured preprocessing pipeline was implemented to prepare the dataset for ML model training. Initially, raw RSSI values from the four APs were converted to absolute values to standardize signal strength measurements, as certain Android hardware APIs may yield readings that fluctuate around zero. This transformation stabilizes the input distribution and mitigates sign-related inconsistencies. For the smartphone inertial data, the three-dimensional accelerometer signals were combined into a magnitude feature using the Euclidean norm calculated as:

$$\text{acc}_{\text{magnitude}} = \sqrt{\text{acc}_x^2 + \text{acc}_y^2 + \text{acc}_z^2}. \quad (1)$$

Zero values in this field were replaced with the mean magnitude of the corresponding human density group to prevent propagation of missing or corrupted data. Missing values in other features were similarly imputed. Finally, a standard Z-score normalization was applied across all features to ensure consistent scaling and compatibility with downstream regression models. The overall preprocessing pipeline, including RSSI transformation, magnitude calculation, imputation, and normalization steps, is summarized in Algorithm 1 and given in Figure 4.

Algorithm 1 RSSI and accelerometer data preprocessing pipeline

Require: Raw dataset \mathcal{D} with RSSI readings, accelerometer measurements, and numberOfPeople

Ensure: Normalized feature matrix \mathbf{X}_{norm}

```

// Raw Data Ingestion
1: Load raw dataset containing RSSI1–RSSI4,  $\text{acc}_x$ ,  $\text{acc}_y$ ,  $\text{acc}_z$ , and numberOfPeople

// RSSI and Accelerometer Preprocessing
2: for each sample  $i$  in  $\mathcal{D}$  do
3:   Compute absolute RSSI values:
4:   for  $k \leftarrow 1$  to 4 do
5:      $\text{RSSI}_k(i) \leftarrow |\text{RSSI}_k(i)|$ 
6:   end for
7:   Compute accelerometer magnitude (Euclidean norm):
8:    $\text{acc}_{\text{mag}}(i) \leftarrow \sqrt{\text{acc}_x(i)^2 + \text{acc}_y(i)^2 + \text{acc}_z(i)^2}$ 
9: end for

// Missing-Value Imputation
10: for each group of samples with equal numberOfPeople do
11:   Impute missing RSSI and  $\text{acc}_{\text{mag}}$  values using group-wise mean
12: end for

// Feature Construction
13: Construct feature matrix:
14:  $\mathbf{X} \leftarrow [\text{RSSI}_1, \text{RSSI}_2, \text{RSSI}_3, \text{RSSI}_4, \text{numberOfPeople}, \text{acc}_{\text{mag}}]$ 

// Feature Normalization
15: for each feature column  $j$  in  $\mathbf{X}$  do
16:   Apply z-score normalization:
17:    $\mathbf{X}_{\text{norm}}(:, j) \leftarrow \frac{\mathbf{X}(:, j) - \mu_j}{\sigma_j}$ 
18: end for
return  $\mathbf{X}_{\text{norm}}$ 

```

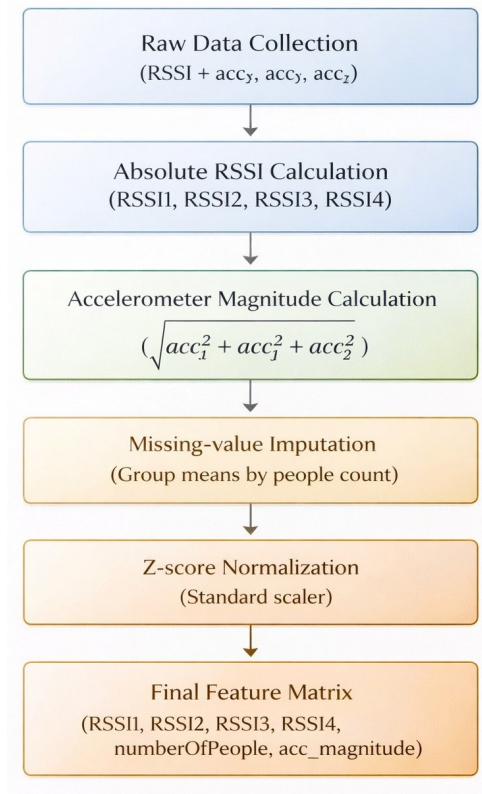


Figure 4: Data preprocessing pipeline.

4.2 Error Computation Using Conventional WLS Localization Method

To quantify localization accuracy, a baseline WLS algorithm was applied to the RSSI observations. This algorithm estimated the location of the measurement point based on known AP coordinates, assuming signal propagation obeyed a simplified path-loss model. Unlike the ordinary least squares approach, WLS assigns a weight to each observation, typically proportional to the inverse of its variance, giving higher importance to more reliable measurements [32]. The WLS position estimate is computed as follows [5].

Let $RSSI_i$ denote the received signal strength indicator measured between the mobile device and the i^{th} AP, where $i = 1, \dots, 4$. According to the log-distance path-loss model [5], [32], the RSSI measurement is expressed as

$$RSSI_i = RSSI(d_0) - 10n \log_{10} \left(\frac{d_i}{d_0} \right) + \epsilon_i, \quad i = 1, \dots, 4 \quad (2)$$

where

- $RSSI(d_0)$ is the mean RSSI value at the reference distance d_0 ,
- n is the path-loss exponent,
- d_i is the true distance between the mobile device and the i^{th} AP,
- ϵ_i represents measurement noise caused by shadowing and multipath propagation.

Following [5], the estimated distance \hat{d}_i is obtained by inverting Equation 2:

$$\hat{d}_i = d_0 10^{\frac{RSSI(d_0) - RSSI_i}{10n}}, \quad i = 1, \dots, 4. \quad (3)$$

The parameters $RSSI(d_0)$ and n are adopted from the literature, consistent with the conventional RSSI-based localization frameworks in [32] and [5].

Let the unknown two-dimensional position of the mobile device be defined as

$$\mathbf{X} = \begin{bmatrix} x \\ y \end{bmatrix}, \tag{4}$$

and the known coordinates of the i^{th} AP be given by

$$\mathbf{S}_i = \begin{bmatrix} x_i \\ y_i \end{bmatrix}, \quad i = 1, \dots, 4. \tag{5}$$

The geometric distance between the mobile device and the i^{th} AP [5], [32] is then expressed as

$$d_i(\mathbf{X}) = \|\mathbf{X} - \mathbf{S}_i\|_2 = \sqrt{(x - x_i)^2 + (y - y_i)^2}. \tag{6}$$

Using the estimated distances \hat{d}_i , the measurement residual for the i^{th} AP is defined as

$$y_i = \hat{d}_i - d_i(\mathbf{X}), \quad i = 1, \dots, 4. \tag{7}$$

Stacking all residuals yields the observation vector [5], [32]

$$\mathbf{y} = [y_1 \quad y_2 \quad y_3 \quad y_4]^T. \tag{8}$$

Following the conventional WLS formulation in [32], [5], the position estimate $\hat{\mathbf{X}}$ is obtained by minimizing the weighted squared residuals:

$$\hat{\mathbf{X}} = \arg \min_{\mathbf{x} = [x, y]^T} (\mathbf{y}^T \mathbf{W} \mathbf{y}) \tag{9}$$

where \mathbf{W} denotes the weighting matrix associated with the distance measurements. Here, the minimization is performed with respect to the two-dimensional position vector $\mathbf{X} = [x, y]^T$, while \mathbf{y} denotes the residual observation vector. In accordance with the conventional WLS approach described in [32], [5], equal weighting is assumed:

$$\mathbf{W} = \mathbf{I}, \tag{10}$$

where \mathbf{I} is the identity matrix.

Since the distance model in Equation (6) is nonlinear with respect to \mathbf{X} , a first-order Taylor series expansion is applied around the current position estimate $\mathbf{X}^{(t)}$ [5], [32]. This yields the linearized observation model

$$\mathbf{y} \approx \mathbf{H} \Delta \mathbf{X}, \tag{11}$$

where

- $\Delta \mathbf{X} = [\Delta x \quad \Delta y]^T$ is the position correction vector,
- \mathbf{H} is the Jacobian (design) matrix.

The i^{th} row of the Jacobian matrix \mathbf{H} [5], [32] is given by

$$\mathbf{H}_i := \begin{bmatrix} \frac{\partial d_i}{\partial x} & \frac{\partial d_i}{\partial y} \end{bmatrix} = \begin{bmatrix} \frac{x - x_i}{d_i(\mathbf{X})} & \frac{y - y_i}{d_i(\mathbf{X})} \end{bmatrix}, \quad i = 1, \dots, 4. \tag{12}$$

The WLS estimate of the correction vector [5], [32] is then computed as

$$\Delta \hat{\mathbf{X}} = (\mathbf{H}^T \mathbf{W} \mathbf{H})^{-1} \mathbf{H}^T \mathbf{W} \mathbf{y}, \tag{13}$$

and the updated position estimate is obtained by

$$\hat{\mathbf{X}} = \mathbf{X}^{(t)} + \Delta \hat{\mathbf{X}}. \tag{14}$$

This solution corresponds to the conventional WLS localization method adopted as the baseline approach in [5], [32].

Let $\mathbf{X}_{gt} = [x_{gt} \ y_{gt}]^T$ denote the known ground-truth position of the mobile device. The localization error is computed as the Euclidean distance between the WLS-estimated position and the ground truth [5], [32]:

$$e = \|\hat{\mathbf{X}} - \mathbf{X}_{gt}\|_2 = \sqrt{(\hat{x} - x_{gt})^2 + (\hat{y} - y_{gt})^2}. \quad (15)$$

For N experimental trials, the mean localization error is calculated as [32]

$$\bar{e} = \frac{1}{N} \sum_{k=1}^N e_k. \quad (16)$$

The error metric was calculated as the Euclidean distance between the true measurement point and the estimated position from WLS. The mean error in the scenario with no people (0 individual in the experimental area) was defined as the reference error. For each other scenario with a different human crowd, the deviation from this reference was computed as:

$$\text{Deviation} = |\text{Error}_{\text{crowded}} - \text{Error}_{\text{reference}}| \quad (17)$$

This deviation was used as the target variable for the three regression models. Table 2 provides the mean WLS localization errors and their corresponding deviations relative to the baseline scenario, highlighting the incremental error introduced by increasing human density.

Table 2: WLS localization errors and corresponding deviations for each human crowd density scenario.

Number of Moving People	Mean WLS Localization Error (m)	Deviation from the Baseline (m)
0	1.405	0.000
4	1.525	0.120
8	1.622	0.217
12	1.730	0.325
16	1.977	0.572
20	2.906	1.501

4.3 Feature Engineering

The final feature vector for ML modeling consists of:

- Normalized RSSI measurements from four APs,
- Human density (number of moving people) and
- Accelerometer magnitude.

Although the smartphone remained stationary during experiments, the accelerometer feature was retained to explore its potential value in a sensor-fusion context. These features were particularly expected to reflect both signal propagation characteristics and moving crowd-induced variations.

The relationships among the extracted features and the target deviation variable are illustrated in Figure 5. The correlation matrix highlights moderate positive correlations between certain RSSI features and deviation while accelerometer magnitude exhibits a slightly low but meaningful correlation due to the stationary nature of the measurements. Although the human density (number of moving people) variable is explicitly available in the controlled dataset used in this study, the proposed framework is not intrinsically dependent on this feature. In practical deployments where the exact number of individuals may not be directly observable, equivalent proxy indicators such as RSSI variance statistics, channel fluctuation metrics, device-side inertial cues, or vision-based crowd estimation mechanisms can be employed to approximate crowd-density effects.

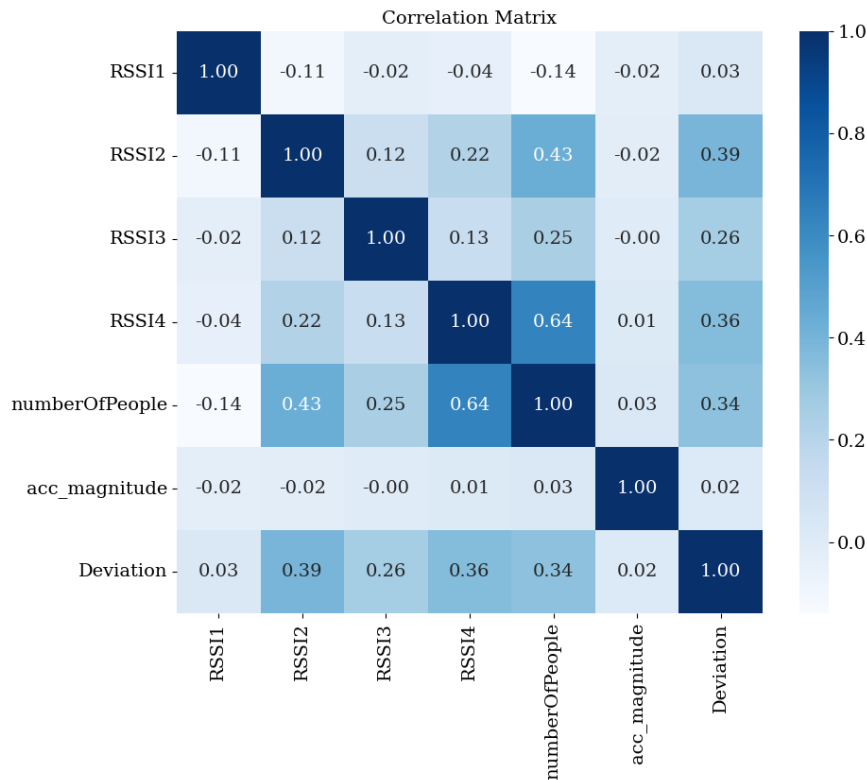


Figure 5: Correlation matrix illustrating the pairwise Pearson correlations among the extracted features (RSSI values, number of moving people, and accelerometer magnitude) and the target deviation variable.

4.4 Modeling Strategy

The proposed ML task was formulated as a regression problem, where the dependent variable was defined as the deviation (in meters) between the baseline WLS localization error and the corresponding crowd scenario. This formulation allowed the ML framework to capture continuous variations in localization error as a function of Wi-Fi signal metrics, moving human density, and inertial sensor features.

To ensure representativeness across moving human density conditions, the dataset was partitioned into training and testing subsets in a stratified manner. The training phase employed five-fold cross-validation, a widely adopted resampling strategy that partitions the data into five folds, iteratively training on four folds while validating on the remaining one. This process mitigates variance in performance evaluation and provides a more reliable estimate of generalization compared to a single train-test split. This solution corresponds to the conventional WLS localization method adopted as the baseline approach in [22].

5 Proposed ML Framework Mitigating Moving Human Crowd Effects for Wi-Fi Indoor Localization

The proposed ML framework is designed to predict deviations in Wi-Fi-based indoor localization accuracy under varying human crowd conditions. Conventional signal modeling approaches such as deterministic path-loss models and stand-alone empirical fingerprinting often struggle in dynamic indoor environments because they cannot fully capture the highly nonlinear effects introduced by moving human presence, multipath propagation, and environmental variability [26], [20].

ML-based techniques offer a promising solution to these difficult challenges to estimate precise indoor localization. Unlike conventional models, ML algorithms are favorably capable of learning complex nonlinear mappings between input features (e.g., RSSI values, inertial sensor data, and crowd density) and localization errors [23]. By leveraging statistical learning principles, ML not only reduces

reliance on hand-crafted propagation models but also adapts to diverse, dynamic and noisy real-world conditions. Prior studies have demonstrated that regression- and ensemble-based ML techniques can significantly enhance indoor localization performance by improving robustness to interference and generalization across instable heterogeneous indoor environments [19].

In this study, the proposed ML framework integrates standardized preprocessing of heterogeneous inputs with supervised regression models to enhance the robustness of Wi-Fi-based indoor localization. Its primary objective is to anticipate and compensate for localization errors primarily arising from moving human-induced signal degradation, while simultaneously providing a practical foundation that can be adapted to real-time precise localization systems for dynamic error correction. By realistically uniting methodological accuracy with practical applicability, the ML framework offers a viable solution for achieving reliable and accurate localization in crowded indoor environments where human presence and movement substantially affect signal stability.

5.1 Framework Overview

The proposed ML framework is structured as a sequential pipeline designed to transform raw experimental measurements into reliable predictions of moving crowd-induced localization errors. It begins with data preprocessing and feature engineering to prepare heterogeneous inputs such as RSSI values, human density levels, and inertial sensor magnitudes. Afterward, supervised regression models are trained using five-fold cross-validation to ensure robustness and mitigate overfitting. Independent testing is then performed to validate model generalization, followed by comparative evaluation of different algorithms using multiple performance metrics. This structured workflow ensures methodological consistency while maintaining practical relevance for real-world indoor localization. The overall architecture of the proposed ML framework, including all stages from preprocessing to comparative evaluation, is summarized in Algorithm 2 and presented in Figure 6.

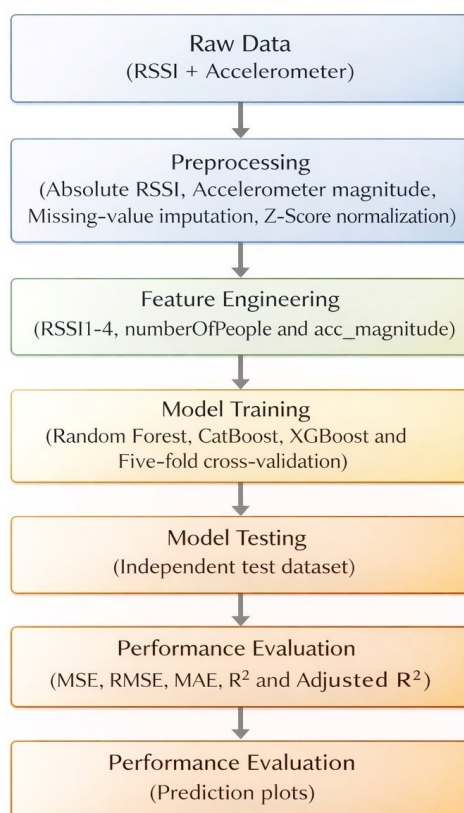


Figure 6: The proposed ML framework pipeline with the sequential steps from raw data acquisition to performance evaluation and interpretation.

Algorithm 2 The proposed ML framework pipeline

Require: Raw RSSI and accelerometer data**Ensure:** Trained models, performance metrics, and prediction plots*// Raw Data Ingestion*

1: Load raw data containing RSSI readings and accelerometer measurements

// Preprocessing

2: Compute absolute values of all RSSI readings

3: Compute accelerometer magnitude $acc_{\text{mag}}(i) \leftarrow \sqrt{acc_x(i)^2 + acc_y(i)^2 + acc_z(i)^2}$ for each sample

4: Impute any missing values in the dataset

5: Normalize all features using z-score normalization

// Feature Engineering

6: Select features (e.g., RSSI1–4, numberOfPeople, acc_mag) for modeling

7: Split data into training set and independent test set

*// Model Training (5-fold Cross-Validation)*8: **for** each model M in {Random Forest, CatBoost, XGBoost} **do**9: Perform 5-fold cross-validation on M using the training set10: Train M on each training fold and validate on the corresponding validation fold11: Retrain M on the entire training set to obtain final model M^* 12: **end for***// Model Testing*13: **for** each trained model M^* **do**14: Use M^* to predict outcomes on the independent test set15: **end for***// Performance Evaluation*16: **for** each model M^* **do**17: Compute performance metrics (MSE, RMSE, MAE, R^2 , adjusted R^2) on test set predictions18: **end for**

19: Summarize and compare all metrics across models

*// Visual Evaluation*20: Generate prediction plots (e.g., actual vs. predicted values) for each model

5.2 Regression Models

In this study, the prediction task was formulated as a regression problem, since the target variable represents a continuous outcome: the deviation (in meters) between the baseline WLS localization error and the error observed under different moving human crowd conditions. Regression models are particularly suited for this type of task as they can successfully capture the quantitative relationship between input features (e.g., RSSI measurements, crowd density and accelerometer magnitude) and a continuous response variable. Unlike classification methods, which predict discrete labels, regression approaches allow precise estimation of error magnitudes, making them ideal for modeling crowd-induced degradation in indoor localization accuracy.

Regression was chosen here since it provides a systematic way to quantify and predict the extent of indoor localization error, rather than only distinguishing between error/no-error cases. This enables anticipatory correction mechanisms, which are essential for real-world indoor localization systems operating in dynamic environments to provide widespread live and user-centered services on demand.

Three regression algorithms utilized in this study, i.e., Random Forest, CatBoost and XGBoost, each offering distinct advantages for modeling non-linear relationships are briefly explained and their

use in this study is justified as follows:

- **Random Forest Regressor (RFR):** It is essentially an ensemble of decision trees constructed through bootstrap aggregating, where random subsets of features are considered at each split. By averaging across many weak learners, RFR mitigates overfitting, effectively captures complex non-linear patterns, and provides stable predictions even in the presence of noisy data [23].

In this study, RFR is used to learn the relationship between RSSI-based features, human crowd density, inertial sensor measurements, and the resulting WLS localization error.

Let the input feature vector be denoted as $\mathbf{x}_i \in \mathbb{R}^d$ and the target output as y_i , representing the localization error obtained from the conventional WLS method. Each regression tree $T_m(\cdot)$ partitions the feature space into disjoint regions and predicts a constant value within each region:

$$T_m(\mathbf{x}) = \sum_l c_{m,l} \mathbb{I}(\mathbf{x} \in R_{m,l}), \quad (18)$$

where $R_{m,l}$ denotes the l^{th} leaf region and $c_{m,l}$ is the mean target value of the samples in that region [29].

To reduce model variance and improve generalization, the forest is constructed using bootstrap aggregation and random feature selection. The final regression output is obtained by averaging the predictions of all trees:

$$\hat{y}(\mathbf{x}) = \frac{1}{M} \sum_{m=1}^M T_m(\mathbf{x}), \quad (19)$$

where M is the number of trees in the ensemble. In the proposed framework, $\hat{y}(\mathbf{x})$ represents the predicted crowd-induced localization error, which is subsequently used to correct the conventional WLS position estimate [29].

- **CatBoost Regressor:** It is a gradient boosting framework specifically designed to handle categorical and heterogeneous features efficiently. Its unique ordered boosting strategy reduces prediction shift and overfitting, while built-in mechanisms address the challenges of mixed-type datasets. A key factor for employing CatBoost is that it has consistently demonstrated strong predictive performance compared to other boosting algorithms, balancing accuracy with ease of implementation [11].

In this study, CatBoost is employed to capture nonlinear and interaction-driven error patterns caused by dynamic human crowd effects in indoor localization.

Given an input feature vector \mathbf{x}_i and target output y_i , the CatBoost prediction is expressed as

$$\hat{y}(\mathbf{x}) = \sum_{m=1}^M \alpha_m T_m(\mathbf{x}), \quad (20)$$

where $T_m(\cdot)$ denotes the m^{th} regression tree and α_m represents its corresponding learning weight. Each tree is trained to fit the residual error of the previous ensemble by minimizing a loss function $\mathcal{L}(y, \hat{y})$ [11].

In the proposed framework, CatBoost benefits from its ordered boosting strategy, which reduces prediction bias and overfitting, making it suitable for modeling structured RSSI distortions under varying crowd densities.

- **XGBoost Regressor:** It is a highly optimized gradient boosting method that incorporates both L1 and L2 regularization to improve generalization and prevent overfitting. Its efficiency lies in parallelized tree construction, scalability to large datasets, and flexible parameter tuning. Due to

its speed and predictive power, XGBoost has become a widely adopted standard for structured ML tasks [14].

The objective function minimized at the t^{th} boosting iteration is defined as

$$\mathcal{J}^{(t)} = \sum_i \mathcal{L}(y_i, \hat{y}_i^{(t-1)} + T_t(\mathbf{x}_i)) + \Omega(T_t), \quad (21)$$

where $\mathcal{L}(\cdot)$ denotes the loss function, $T_t(\cdot)$ is the newly added regression tree, and $\Omega(\cdot)$ is a regularization term that penalizes tree complexity [14].

By explicitly incorporating regularization, XGBoost effectively models crowd-induced localization errors while maintaining robustness against overfitting, especially under heterogeneous RSSI and sensor conditions.

These three algorithms were chosen for their established effectiveness on tabular datasets with complex, non-linear structures, their resilience to moderate inter-feature correlations, and their ability to model subtle patterns underlying signal degradation, human presence and human mobility effects. The hyperparameters of each regressor were initially configured to widely adopted default values, as shown in Table 3, thereby establishing a transparent baseline for comparison and ensuring reproducibility in subsequent evaluations and potential further optimization [10].

Table 3: Hyperparameter settings used for the ML regressors in the proposed framework.

Model	n_estimators	max_depth	learning_rate	random_state	Other
Random Forest	100 (default)	None	–	42	–
CatBoost	1000 (default)	6 (default)	0.03 (default)	42	Verbose = 0
XGBoost	100	4	0.3 (default)	42	–

5.3 Training and Cross-Validation

To ensure reliable evaluation, a five-fold cross-validation strategy was applied in this study, widely preferred to mitigate overfitting and obtain stable performance estimates on moderate datasets. Model accuracy was assessed using multiple regression metrics that capture complementary aspects of predictive performance. Mean Squared Error (MSE) and Root Mean Squared Error (RMSE) were used to evaluate the magnitude of squared errors, while Mean Absolute Error (MAE) provided a more interpretable measure of average deviation less affected by outliers [13]. To assess explanatory power, the Coefficient of Determination (R^2) and Adjusted R^2 were included, with the latter correcting for predictor count to avoid overestimation. In addition, percentage-based measures such as Mean Absolute Percentage Error (MAPE) and Symmetric Mean Absolute Percentage Error (SMAPE) were adopted to compare relative errors and address instability near zero values [9].

Let $\{(y_i, \hat{y}_i)\}_{i=1}^N$ denote the ground-truth targets and the corresponding model predictions on a validation/test set, where N is the number of samples. The prediction error is defined as $e_i = y_i - \hat{y}_i$. The performance metrics [9] used in this study are defined as follows:

$$\text{MSE} = \frac{1}{N} \sum_{i=1}^N (y_i - \hat{y}_i)^2 \quad (22)$$

$$\text{RMSE} = \sqrt{\frac{1}{N} \sum_{i=1}^N (y_i - \hat{y}_i)^2} \quad (23)$$

$$\text{MAE} = \frac{1}{N} \sum_{i=1}^N |y_i - \hat{y}_i| \quad (24)$$

Let $\bar{y} = \frac{1}{N} \sum_{i=1}^N y_i$. Then,

$$R^2 = 1 - \frac{\sum_{i=1}^N (y_i - \hat{y}_i)^2}{\sum_{i=1}^N (y_i - \bar{y})^2}. \quad (25)$$

For d input features (predictors),

$$R_{\text{adj}}^2 = 1 - \left(1 - R^2\right) \frac{N - 1}{N - d - 1} \quad (26)$$

$$\text{MAPE} = \frac{100}{N} \sum_{i=1}^N \left| \frac{y_i - \hat{y}_i}{y_i} \right| \quad (27)$$

where y_i and \hat{y}_i denote the ground-truth value and the predicted value of the i th sample, respectively [9].

$$\text{SMAPE} = \frac{100}{N} \sum_{i=1}^N \frac{|y_i - \hat{y}_i|}{(|y_i| + |\hat{y}_i|) / 2} \quad (28)$$

In the five-fold cross-validation procedure, MAPE and SMAPE [9] are computed for each fold and reported as the average values across folds, similar to the other regression performance metrics.

In this study, the hyperparameters of the regression models were primarily initialized with widely adopted default or near-default configurations to ensure methodological transparency and reproducibility across algorithms. Given the moderate dataset size and the comparative nature of the analysis, exhaustive hyperparameter tuning was intentionally avoided to reduce the risk of overfitting and model-specific bias. Nevertheless, systematic optimization strategies such as grid search, random search, or Bayesian optimization may further refine predictive performance, particularly in larger or more heterogeneous datasets. Future work will investigate adaptive hyperparameter tuning mechanisms and automated search strategies to assess their impact on generalization capability. Preliminary exploratory tuning experiments conducted during pilot analyses indicated only marginal performance gains under the present dataset scale, which reinforced the decision to preserve default configurations for methodological transparency.

6 Evaluation and Validation

This section presents the performance evaluation of the proposed ML models using both cross-validation and independent test data. Multiple regression metrics were employed to quantify the accuracy, robustness, and generalizability of each model.

6.1 Cross-Validation Results

To ensure robust evaluation of the regression models and reduce the risk of overfitting, a five-fold cross-validation strategy was adopted during training. This approach iteratively trains on four folds while validating on the remaining one, with the process repeated five times, thereby preserving the distribution of moving human density scenarios across folds and ensuring fair comparisons under varying crowd conditions.

The performance of the Random Forest, CatBoost and XGBoost regressors was assessed using standard regression metrics, with MSE and RMSE serving as the primary indicators of predictive accuracy. The cross-validation results are summarized in Table 4, which reports the average MSE and RMSE across folds. As shown, CatBoost achieved the lowest average error (MSE = 0.0218, RMSE = 0.1477), closely followed by Random Forest (MSE = 0.0229, RMSE = 0.1513), while XGBoost exhibited comparatively higher errors (MSE = 0.0478, RMSE = 0.2186).

These findings confirm that ensemble-based tree models, particularly CatBoost, are more effective at capturing the non-linear effects of moving human-induced signal fluctuations. Overall, the results show that the models not only have learned meaningful patterns in the data and but also exhibit strong generalization capability, even in the presence of moderate feature correlation.

Table 4: Average five-fold cross-validation performance of the regression models.

Model	Five-Fold Mean MSE (m ²)	Five-Fold Mean RMSE (m)
Random Forest	0.0229	0.1513
CatBoost	0.0218	0.1477
XGBoost	0.0478	0.2186

6.2 Test Set Evaluation

Following model training, the final Random Forest, CatBoost, and XGBoost models were evaluated on an independent test set collected under similar conditions but with a crowd density of three individuals, a scenario not included in the training data. This setting was chosen deliberately to examine the ability of the models to interpolate to unseen moving human density levels and thus test their robustness.

Model performance was quantified using six regression metrics: MSE, RMSE, MAE, R^2 , Adjusted R^2 and SMAPE. While conventional MAPE was also considered initially, it produced unrealistically high values because the denominator approaches zero when deviations are very small. This leads to instability in percentage-based error measures. To address this issue, SMAPE was rather employed, as symmetrically normalizing the absolute error and avoiding inflation in cases where the actual values are close to zero.

The evaluation results obtained during the model training phase are summarized in Table 4, while the generalization performance on an independent test set with three moving individuals is visualized in Figure 7 as a heatmap. Among the three models, CatBoost achieved the lowest RMSE (0.331) and the highest R^2 (0.926), demonstrating superior generalization capability. Random Forest performed moderately well across all metrics, whereas XGBoost exhibited the highest SMAPE (38.66%), indicating greater variability in percentage-based errors. Overall, the results confirm that ensemble-based regressors are capable of capturing meaningful patterns in the data, with CatBoost showing the most reliable performance under moving crowd-induced signal degradation.

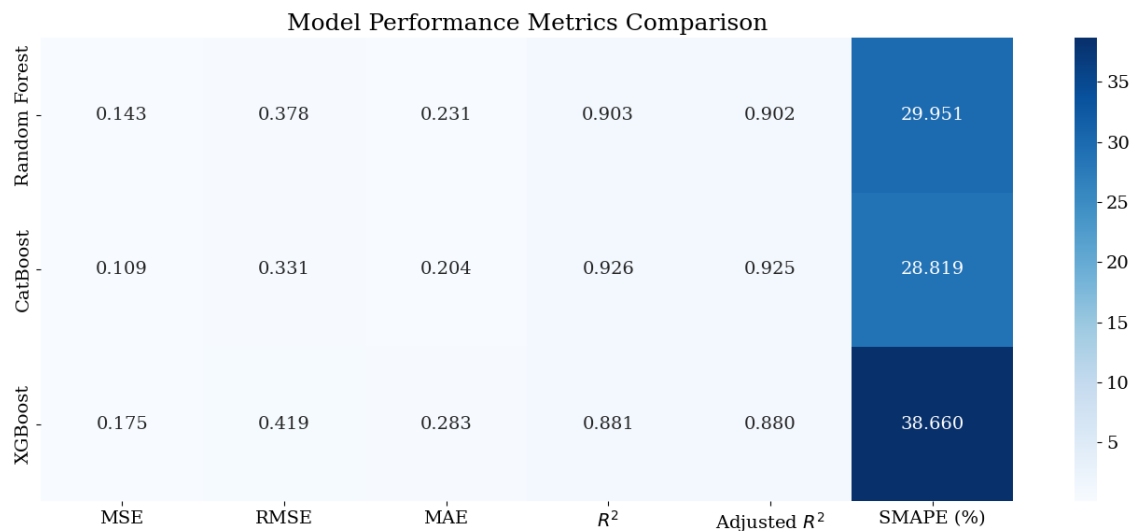


Figure 7: Heatmap comparison of test set performance metrics across the regression models.

Figure 8 shows the comparison of predicted deviations by the Random Forest, CatBoost and XGBoost regressors against the actual deviation values observed in the independent test dataset. The x-axis represents the individual test samples, while the y-axis indicates the magnitude of the deviation (in meters).

From the figure, it is evident that all three models follow the general trend of the true deviations, capturing both small and large fluctuations in localization error. However, differences emerge in their predictive stability. CatBoost (green squares) most closely aligns with the actual deviations (blue circles), particularly in scenarios with moderate error magnitudes, which directly corresponds to its

superior RMSE and R^2 values reported earlier. Random Forest (orange crosses) also performs reasonably well but exhibits slight underfitting in high-deviation peaks, leading to moderate accuracy. On the other hand, XGBoost (red triangles) tends to overshoot at several high-error points, demonstrating higher sensitivity to outliers and greater variance in its predictions.

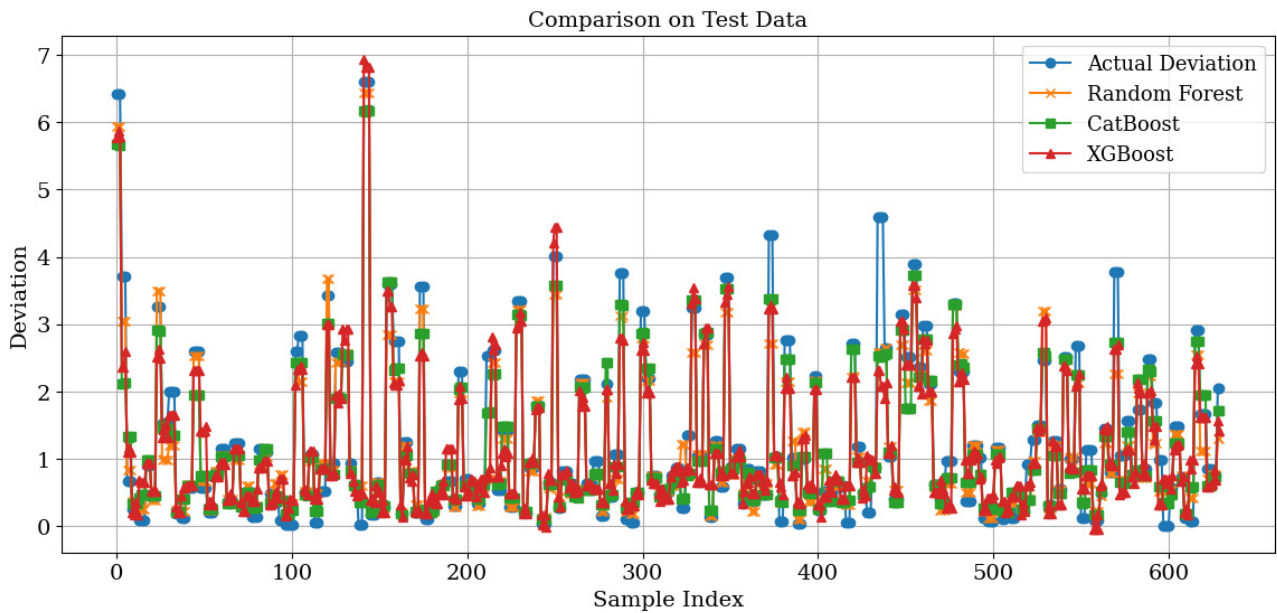


Figure 8: Comparison of actual deviation and predicted values for the test dataset.

The independent test set performance of the three regression models is illustrated in Figure 9, where RMSE and R^2 values are compared. The results confirm the quantitative findings and highlight the relative strengths of each algorithm. Among the three tested regressors, CatBoost achieved the lowest RMSE (0.331 m) and the highest R^2 (0.926), demonstrating superior generalization capability and robustness in modeling non-linear fluctuations induced by moving human presence. Random Forest followed closely, with a slightly higher RMSE (0.378 m) while maintaining strong explanatory power ($R^2 = 0.903$), indicating that it remains a competitive alternative. In contrast, XGBoost exhibited the weakest performance, with the highest RMSE (0.419 m) and the lowest R^2 (0.881), suggesting reduced effectiveness in capturing the complex variability of Wi-Fi signals under moving human crowd interference.

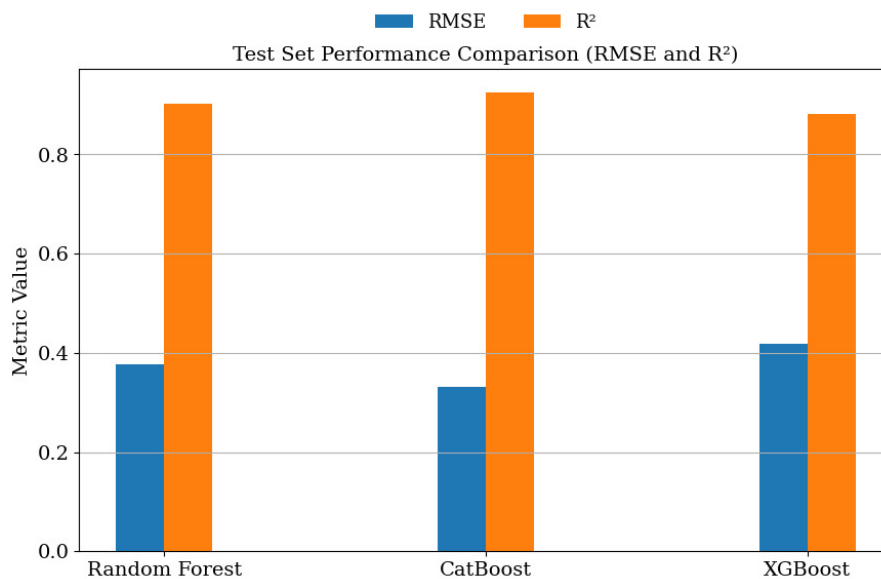


Figure 9: Comparison of crowd-induced error reduction performance on the test dataset.

7 Results and Discussion

This section analyzes the results obtained from the three regression models trained to predict moving human-crowd-induced degradation in Wi-Fi-based indoor localization accuracy. The evaluation was performed on an independent test set collected under similar environmental conditions but at different time slots to assess the generalization capability of the models.

7.1 Reference Error and Deviation Behavior Across Moving Human Crowd Levels

The zero-person mean WLS localization error is 1.405 m and is taken as the reference. As moving human crowd size increases, both the mean WLS localization error and the deviation from the reference grow in an approximately monotonic manner. Table 2 reports, for each moving human crowd level, the mean WLS localization error (m) and the corresponding deviation from the reference (m). The increases are moderate at four and eight people (+8.5% and +15.4% respectively), and become more pronounced at twelve and sixteen people (+23.1% and +40.7% respectively). In the twenty people scenario, the error rises to 2.906 m, the deviation reaches 1.501 m, and the relative increase jumps to +106.8%. This results clearly indicate that as moving human density increases, the combined effects of shadowing, absorption and multipath (and beyond a certain threshold, the disruption of line-of-sight continuity) can amplify localization error in a non-linear manner.

The rise of percentage increases across all moving human crowd levels is summarized in Figure 10. The figure shows a gradual degradation at low-to-moderate human crowd densities and a sharp jump at high human crowd density. These findings confirm that RSSI-based multilateration is highly moving crowd-sensitive even under controlled, stationary-device conditions, and they motivate the need for the proposed ML-based error-compensation layer (moving human crowd-aware correction) presented in the paper for precise indoor localization.

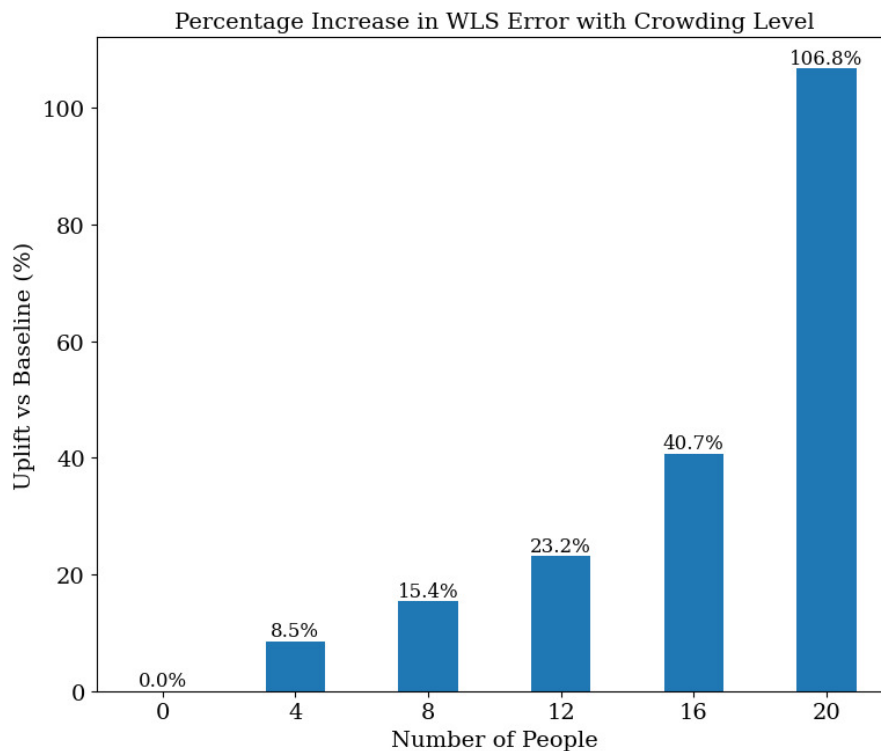


Figure 10: Percentage increase in WLS localization error relative to the 0-person baseline (1.405 m) across moving human crowd levels.

7.2 Crowd-Aware Error Compensation Performance of CatBoost-Based WLS Refinement

The results confirm that the baseline WLS localization error increases as moving human crowd density rises while the proposed moving human crowd-aware CatBoost-based error prediction and compensation layer models and corrects the WLS-induced deviation, yielding a substantial reduction in localization error. On the independent test set with an unseen three-person density, CatBoost achieved $\text{RMSE} = 0.331$ m and $R^2 = 0.926$, corresponding to an improvement of approximately 76.5% relative to the zero-person WLS reference error (1.405 m).

A comparative distribution analysis corroborates the above findings. In Figure 11, the Cumulative Distribution Function (CDF) of the post-CatBoost residuals shifts markedly left (toward lower errors) compared to baseline WLS, indicating improvements not only in the mean but also at the median, and the upper percentiles (e.g., the 95th). These results state that moving human crowd-induced deviation can be learned in a predictable manner, and that CatBoost, by capturing the threshold effect emerging at high human crowd densities, enhances the robustness of WLS-based localization.

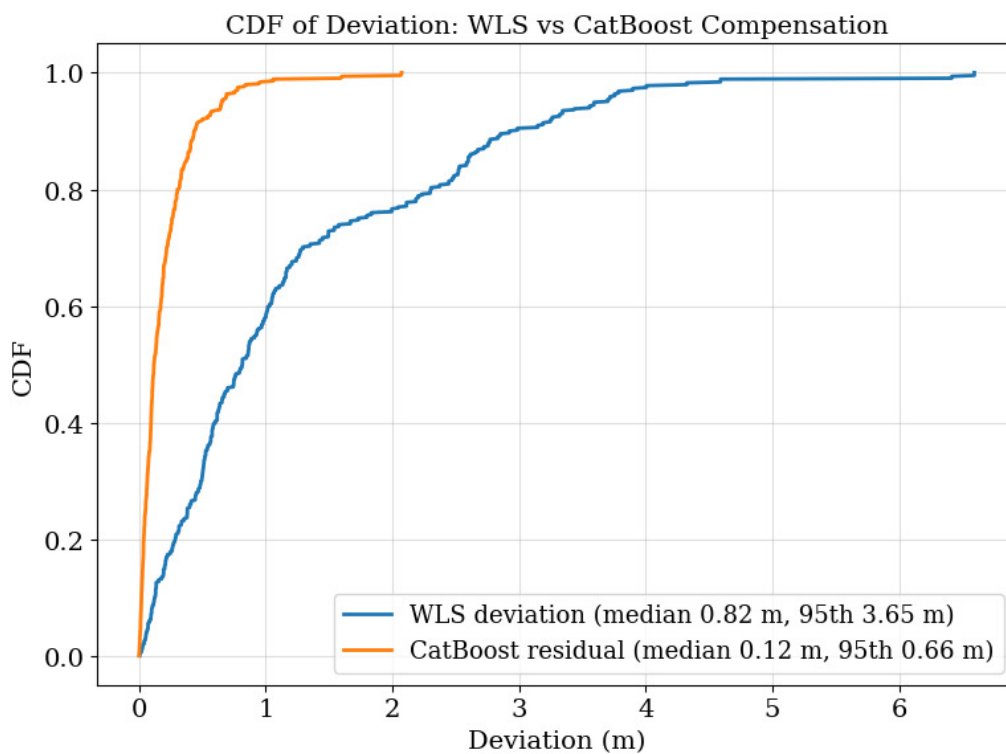


Figure 11: CDF of Localization Deviation for baseline WLS and CatBoost

Figure 12 shows that as moving human crowd level increases, the mean WLS localization error rises whereas the proposed CatBoost-based compensation layer reduces the mean error markedly at all human crowd levels. The percentage labels on the graph report the magnitude of the reduction relative to baseline WLS:

- 93.9% at zero people (1.405 m \rightarrow 0.086 m),
- 86.6% at four people (1.525 m \rightarrow 0.205 m),
- 84.7% at eight people (1.622 m \rightarrow 0.248 m),
- 86.0% at twelve people (1.730 m \rightarrow 0.242 m),
- 86.0% at sixteen people (1.977 m \rightarrow 0.277 m), and
- 89.4% at twenty people (2.906 m \rightarrow 0.290 m).

This resulting pattern highlights two key points: (i) the relative gain is high at every moving human crowd level (85–94%), and (ii) the absolute gain grows with moving human crowd density; for example, at twenty people the reduction compared with baseline WLS is about 2.62 m. Notably, the post-compensation residual localization error remains within the 0.09–0.29 m band across all human crowd densities, indicating stable performance against moving human crowd-induced variability. In addition to these enhanced results, the subsequent facts presented through Figure 9 are consistent with the distribution-level results in Figure 11 and align with the independent test performance (RMSE = 0.331 m, $R^2 = 0.926$), confirming that the proposed CatBoost moving human crowd-aware layer delivers systematic, meter-scale improvements over baseline WLS-based localization.

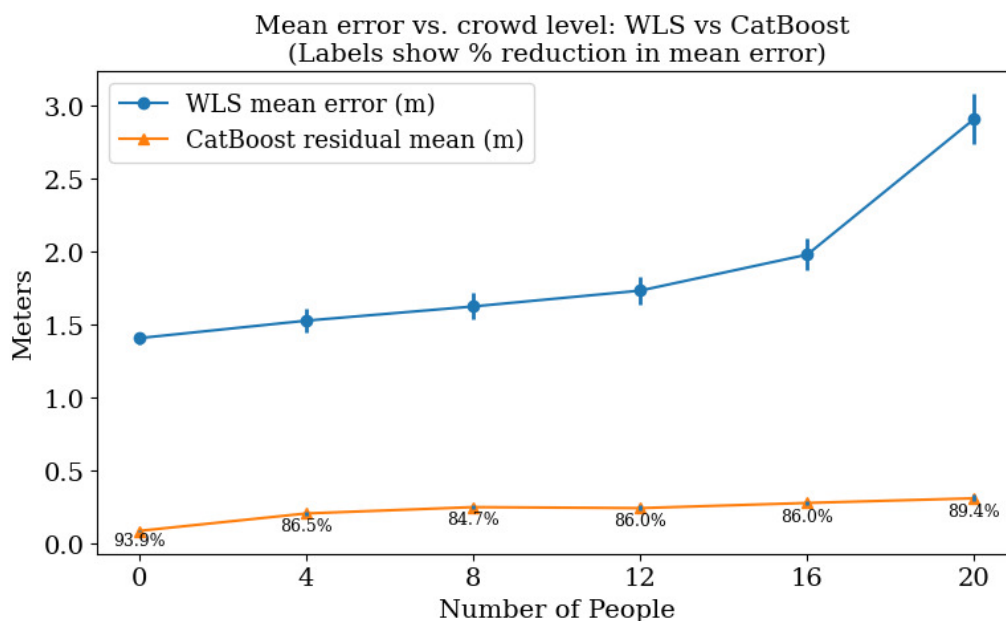


Figure 12: Mean error (m) vs. moving human crowd level: WLS (before) and CatBoost (after)

Although the accelerometer data was included in all models, the gain in accuracy was marginal but meaningful in nature, which is likely due to the fact that the measurement device remained stationary during all data collection sessions. In more dynamic settings involving device movement or user mobility, inertial features could provide a more substantial contribution. In this context, the proposed framework is not designed to optimize sensor fusion for absolute position estimation, but rather to operate as a learning-based error compensation layer, where the regression target represents the deviation of a model-based multilateration estimate from a crowd-free baseline. Within this formulation, isolating or removing individual input modalities would alter the physical meaning of the prediction task rather than provide additional insight into the correction mechanism. Consequently, crowd-induced RSSI dynamics constitute the dominant source of localization degradation in this study, and the evaluation prioritizes robustness and generalization across varying human crowd densities rather than modality-level ablation.

In summary, the results demonstrate that the proposed ML models, particularly CatBoost, can effectively estimate the degree of indoor localization degradation caused by varying human densities. The findings support the potential of sensor-augmented predictive modeling for adaptive indoor localization systems.

Although accelerometer-derived features were included in all regression models, their quantitative contribution remained limited due to the stationary measurement setup. Under such conditions, RSSI dynamics and crowd-density variations represent the primary sources of localization degradation and therefore dominate the predictive learning process. Conceptually, RSSI measurements provide direct information about signal attenuation and multipath fluctuations, while the crowd-density indicator captures the macroscopic environmental factor influencing signal stability. In contrast, accelerometer magnitude mainly reflects micro-level vibrations or minor device disturbances, which become more

informative in mobile-device or user-movement scenarios. From a conceptual ablation perspective, removing RSSI features would significantly reduce the model’s predictive capacity, whereas excluding accelerometer features would lead to only marginal performance differences in the present stationary setup. Nevertheless, retaining inertial cues preserves the framework’s extensibility toward dynamic use cases where user motion, orientation changes, and step-level dynamics are expected to play a more substantial role.

Although the present study primarily focuses on modeling crowd-induced localization deviations rather than system-level deployment, the computational complexity of the employed regression models remains moderate at inference time. Ensemble tree-based regressors Random Forest and CatBoost perform prediction through a limited number of tree traversals, which typically incurs millisecond-level latency on modern smartphones. Since the proposed framework operates as a lightweight post-processing layer over a conventional multilateration baseline, it does not introduce iterative optimization or high-dimensional neural inference overhead. Consequently, the approach is compatible with real-time indoor localization pipelines where RSSI scanning intervals are commonly in the order of hundreds of milliseconds to seconds. In practical deployments, model compression, tree-depth constraints, or edge-side execution strategies can further reduce latency. These characteristics indicate that the proposed learning-based error-compensation layer is computationally feasible for real-time ILS applications without imposing significant hardware requirements.

7.3 Limitations and Future Work

While the proposed framework demonstrates strong performance under controlled experimental conditions, its limitations should be acknowledged. First, the experiments were conducted in a single indoor environment with a fixed spatial layout and a predefined AP configuration, which may limit direct generalization to larger, structurally more complex buildings or different AP geometries and signal propagation characteristics. Second, the localization measurements were collected at a single fixed point with a stationary smartphone, allowing the isolation of moving human crowd effects but not fully capturing user mobility-induced dynamics, orientation variability, or spatial diversity arising from different user positions within the environment.

Extending the framework to mobile-device scenarios introduces additional challenges such as motion-induced sensor noise, device orientation changes, temporal signal drift, and continuously varying signal geometry, which may require more advanced sensor fusion and sequence-aware modeling strategies. Furthermore, scaling the approach to multiple measurement points, heterogeneous AP layouts, or multi-floor environments would increase data heterogeneity and may necessitate adaptive, domain-adaptation, or transfer-learning mechanisms. Another practical consideration is the explicit `NumberOfPeople` feature employed in this study, which may not be directly observable in real-world deployments. However, the proposed learning-based error-compensation framework is not intrinsically dependent on this explicit variable and can instead operate with proxy indicators such as RSSI variance statistics, channel fluctuation metrics, inertial sensor cues, or external crowd-estimation mechanisms derived from infrastructure- or vision-based sensing.

These limitations are not inherent to the proposed learning-based error-compensation concept but rather stem from the deliberate experimental design adopted to isolate crowd-induced RSSI distortions under controlled conditions. Future work will address these challenges by incorporating mobile user trajectories, additional inertial sensors, explicit multi-position validation across diverse user locations, multi-layout datasets, and implicit crowd-density estimation techniques to enhance spatial generalization and deployment realism.

8 Conclusions

This study presented an ML-based approach to predict moving human crowd-induced degradation in Wi-Fi RSSI-based indoor localization systems. An experimental dataset was collected from a controlled $8\text{ m} \times 16\text{ m}$ indoor environment under varying human crowd density scenarios, with RSSI and inertial sensor data recorded at a fixed centered location by using a custom-developed mobile application. The conventional WLS algorithm was used to calculate reference localization errors, and the

deviation caused by moving human presence was modeled using ensemble regressors. The proposed learning-based compensation module is inherently independent of the underlying multilateration solver and can be seamlessly integrated with any model-based indoor localization technique. On the other hand, unlike fingerprinting-based approaches, this study preserves a purely model-based multilateration framework and introduces a lightweight regression-based error correction layer to compensate for human-crowd-induced RSSI distortions.

Among the evaluated three models, CatBoost demonstrated the best performance in terms of RMSE and R^2 , suggesting its suitability for modeling non-linear interactions between signal strength, moving human density, and sensor-derived features. Without compensation, the WLS reference error grows from 1.405 m at zero people to 2.906 m at twenty people, an increase of +106.8%, with a deviation of 1.501 m from the zero-people baseline. With compensation, CatBoost on an independent test set with an unseen three-people density attains RMSE = 0.331 m and $R^2 = 0.926$, representing a 76.5% improvement relative to the zero-people WLS baseline (1.405 m). Across the canonical moving human crowd levels, the post-compensation mean error remains in the 0.09–0.29 m band, with per-level reductions of 93.9% (zero people), 86.6% (four people), 84.7% (eight people), 86.0% (twelve people), 86.0% (sixteen people), and 89.4% (twenty people); for example, at twenty people the WLS mean error drops from 2.906 m to 0.290 m (absolute decrease 2.62 m). The leftward shift of the CDF also confirms improvements beyond the mean, including the median and upper quantiles.

These obtained results indicate that moving human crowd-induced error follows a predictable pattern that can be modeled and corrected by the proposed supervised ML, turning human crowd density-driven variability into lower and more stable meter-level localization errors. In stationary-device trials, accelerometer features yielded marginal added value, which is consistent with limited motion, but the proposed ML framework remains sensor-fusion ready for dynamic use cases.

Future work will explore following directions:

- Conducting experiments in dynamic scenarios where the device or user is in motion.
- Integrating gyroscope and magnetometer readings to further enhance prediction fidelity.
- Expanding the spatial scale and incorporating multiple measurement points to model spatial variance.

The findings indicate that ML models can serve not only as predictive tools for indoor localization accuracy but also as early-warning mechanisms in environments prone to moving human-induced signal variability. This can be especially beneficial in real-time location-based services, where anticipating degradation can lead to more adaptive localization strategies.

Acknowledgments

This research was funded by the Scientific Research Funding Program of Bandirma Onyedi Eylul University, Turkey under project number BAP-24-1003-006.

The authors would like to thank E. Petek, E. Bas and other final-year Computer Engineering students of Bandirma Onyedi Eylul University for their invaluable support in the project.

The authors used an AI-based language assistance tool only for grammatical editing and stylistic refinement. All scientific content, methodology, analysis, and conclusions are entirely the responsibility of the authors.

Data Availability Statement

The experimental dataset generated during the proposed ML-based study is openly available in the Zenodo repository at <https://doi.org/10.5281/zenodo.17179554>. The dataset includes the raw measurements obtained from the experimental setup, along with preprocessed files used for the analyses. These resources are freely accessible for verification, replication and further research by readers.

References

- [1] Ahmad, N.A.; Sahibuddin, S.; Dziyauddin, R.A. (2020). Modelling the effect of human body around user on signal strength and accuracy of indoor positioning, *International Journal of Integrated Engineering*, 12, 72–80, 2020. DOI: <https://doi.org/10.30880/ijie.2020.12.07.008>
- [2] Alfahad, O.; Saied, H.; Malaekah, E.; Rashdi, A.A.; Emam, M.; Bakouri, M. (2025). An auto-adjusting algorithm to enhance indoor localization accuracy: A real-time experimental analysis, *IEEE Access*, 13, 1–12, 2025. DOI: <https://doi.org/10.1109/ACCESS.2025.3541796>
- [3] Alshami, I.H.; Ahmad, N.A.; Sahibuddin, S.; Firdaus, F. (2017). Adaptive indoor positioning model based on WLAN-fingerprinting for dynamic and multi-floor environments, *Sensors*, 17, 1789, 2017. DOI: <https://doi.org/10.3390/s17081789>
- [4] Alvarez-Merino, C.S.; Khatib, E.J.; Muñoz, A.T.; Barco, R. (2025). Integrating indoor localisation technologies for enhanced smart education: Challenges, innovations, and applications, *IEEE Access*, 13, 1–12, 2025. DOI: <https://doi.org/10.1109/ACCESS.2025.3578718>
- [5] Bandirmali, N.; Torlak, M. (2017). ERLAK: On the cooperative estimation of the real-time RSSI based location and k constant term, *Wireless Personal Communications*, 95, 3923–3932, 2017. DOI: <https://doi.org/10.1007/s11277-017-4032-7>
- [6] Basri, C.; El Khadimi, A. (2016). Survey on indoor localization system and recent advances of WiFi fingerprinting technique, In *Proceedings of the 5th International Conference on Multimedia Computing and Systems (ICMCS)*, Marrakech, Morocco, 29 September–1 October 2016; pp. 253–259, 2016. DOI: <https://doi.org/10.1109/ICMCS.2016.7905633>
- [7] Biswas, D.; Barai, S. (2024). Reliable positioning-based human activity recognition based on indoor RSSI changes, *Wireless Networks*, 30, 2917–2937, 2024. DOI: <https://doi.org/10.1007/s11276-024-03712-6>
- [8] Booranawong, A.; Sengchuai, K.; Jindapetch, N. (2019). Implementation and test of an RSSI-based indoor target localization system: Human movement effects on the accuracy, *Measurement*, 133, 370–382, 2019. DOI: <https://doi.org/10.1016/j.measurement.2018.10.031>
- [9] Chicco, D.; Warrens, M.J.; Jurman, G. (2021). The coefficient of determination R^2 is more informative than SMAPE, MAE, MAPE, MSE and RMSE in regression analysis evaluation, *PeerJ Computer Science*, 7, e623, 2021. DOI: <https://doi.org/10.7717/peerj-cs.623>
- [10] Hackeling, G. (2017). *Mastering Machine Learning with scikit-learn*, Packt Publishing Ltd., 2017.
- [11] Ibrahim, A.A.; Ridwan, R.L.; Muhammed, M.M.; Abdulaziz, R.O.; Saheed, G.A. (2020). Comparison of the CatBoost classifier with other machine learning methods, *International Journal of Advanced Computer Science and Applications*, 11, 738–748, 2020. DOI: <https://doi.org/10.14569/IJACSA.2020.0111190>
- [12] Jiao, J.; Li, F.; Deng, Z.; Ma, W. (2017). A smartphone camera-based indoor positioning algorithm of crowded scenarios with the assistance of deep CNN, *Sensors*, 17, 704, 2017. DOI: <https://doi.org/10.3390/s17040704>
- [13] Kamble, V.B.; Deshmukh, S.N. (2017). Comparison between accuracy and MSE, RMSE by using proposed method with imputation technique, *Oriental Journal of Computer Science and Technology*, 10, 773–779, 2017. DOI: <http://dx.doi.org/10.13005/ojcs/10.04.11>
- [14] Lai, S.B.S.; Shahri, N.H.N.B.M.; Mohamad, M.B.; Rahman, H.A.B.A.; Rambli, A.B. (2021). Comparing the performance of AdaBoost, XGBoost, and Logistic Regression for Imbalanced Data, *Mathematics and Statistics*, 9(3), 379–385, 2021. DOI: <https://doi.org/10.13189/ms.2021.090320>

- [15] Leitch, S.G.; Ahmed, Q.Z.; Abbas, W.B.; Hafeez, M.; Laziridis, P.I.; Surephong, P.; Alade, T. (2023). On indoor localization using Wi-Fi, BLE, UWB, and IMU technologies, *Sensors*, 23, 8598, 2023. DOI: <https://doi.org/10.3390/s23208598>
- [16] Liu, J.; Yang, Z.; Zlatanova, S.; Li, S.; Yu, B. (2025). Indoor localization methods for smartphones with multi-source sensors fusion: Tasks, challenges, strategies, and perspectives, *Sensors*, 25, 1806, 2025. DOI: <https://doi.org/10.3390/s25061806>
- [17] Mocanu, I.; Scarlat, G.; Rusu, L.; Pandelica, I.; Cramariuc, B. (2018). Indoor localisation through probabilistic ontologies, *International Journal of Computers Communications & Control*, 13(6), 988–1006, 2018. DOI: <https://doi.org/10.15837/ijccc.2018.6.3022>
- [18] Moayeri, N.; Ergin, M.O.; Lemic, F.; Handziski, V.; Wolisz, A. (2016). PerfLoc (Part 1): An extensive data repository for development of smartphone indoor localization apps, In *Proceedings of the IEEE 27th Annual International Symposium on Personal, Indoor, and Mobile Radio Communications (PIMRC)*, 2016; pp. 1–7. DOI: <https://doi.org/10.1109/PIMRC.2016.7794983>
- [19] Narasimman, S.C.; Alphones, A. (2024). DumbLoc: Dumb indoor localization framework using Wi-Fi fingerprinting, *IEEE Sensors Journal*, 24, 14623–14630, 2024. DOI: <https://doi.org/10.1109/JSEN.2024.3374415>
- [20] Nessa, A.; Adhikari, B.; Hussain, F.; Fernando, X.N. (2020). A survey of machine learning for indoor positioning, *IEEE Access*, 8, 214945–214965, 2020. DOI: <https://doi.org/10.1109/ACCESS.2020.3039271>
- [21] Nomura, A.; Sugasaki, M.; Tsubouchi, K.; Nishio, N.; Shimosaka, M. (2023). Device-free multi-person indoor localization using the change of ToF, In *Proceedings of the IEEE International Conference on Pervasive Computing and Communications (PerCom)*, 2023; pp. 190–199. DOI: <https://doi.org/10.1109/PERCOM56429.2023.10099384>
- [22] Nti, I.K.; Nyarko-Boateng, O.; Aning, J. (2021). Performance of machine learning algorithms with different K values in K-fold cross-validation, *International Journal of Information Technology and Computer Science*, 13, 61–71, 2021. DOI: <https://doi.org/10.5815/ijitcs.2021.06.05>
- [23] Ouameur, M.A.; Caza-Szoka, M.; Massicotte, D. (2020). Machine learning enabled tools and methods for indoor localization using low power wireless network, *Internet of Things*, 12, 100300, 2020. DOI: <https://doi.org/10.1016/j.iot.2020.100300>
- [24] Panja, A.K.; Sasidhar, K.; Roy, M.; Chowdhury, C. (2025). A survey on crowd behavior analysis through indoor localization, *Journal of Location Based Services*, 1–40, 2025. DOI: <https://doi.org/10.1080/17489725.2025.2499592>
- [25] Poulouse, A.; Han, D.S. (2019). Hybrid indoor localization using IMU sensors and smartphone camera, *Sensors*, 19, 5084, 2019. DOI: <https://doi.org/10.3390/s19235084>
- [26] Roy, P.; Chowdhury, C. (2021). A survey of machine learning techniques for indoor localization and navigation systems, *Journal of Intelligent and Robotic Systems*, 101, 63, 2021. DOI: <https://doi.org/10.1007/s10846-021-01327-z>
- [27] Roy, P.; Chowdhury, C. (2022). A survey on ubiquitous WiFi-based indoor localization system for smartphone users from implementation perspectives, *CCF Transactions on Pervasive Computing and Interaction*, 4, 298–318, 2022. DOI: <https://doi.org/10.1007/s42486-022-00089-3>
- [28] Salamah, A.H.; Tamazin, M.; Sharkas, M.A.; Khedr, M. (2016). An enhanced WiFi indoor localization system based on machine learning, In *Proceedings of the International Conference on Indoor Positioning and Indoor Navigation (IPIN)*, 2016; pp. 1–8. DOI: <https://doi.org/10.1109/IPIN.2016.7743586>
- [29] Segal, M.R. (2004). Machine learning benchmarks and random forest regression, 2004.

- [30] Singh, N.; Choe, S.; Punmiya, R. (2021). Machine learning based indoor localization using Wi-Fi RSSI fingerprints: An overview, *IEEE Access*, 9, 127150–127174, 2021. DOI: <https://doi.org/10.1109/ACCESS.2021.3111083>
- [31] Syazwani, N.C.J.; Wahab, N.H.A.; Sunar, N.; Ariffin, S.H.S.; Wong, K.Y.; Aun, Y. (2022). Indoor positioning system: A review, *International Journal of Advanced Computer Science and Applications*, 13(6), 477–490, 2022. DOI: <http://dx.doi.org/10.14569/IJACSA.2022.0130659>
- [32] Tarrio, P.; Bernardos, A.M.; Casar, J.R. (2011). Weighed least squares techniques for improved received signal strength based localization, *Sensors*, 11(9), 8569–8592, 2011. DOI: <https://doi.org/10.3390/s110908569>
- [33] Tekkol, T.; Ertürk, N.B. (2024). A new location estimation error minimization model based on Wi-Fi and mobile phone for indoor mobile nodes considering human population, In *Proceedings of the 15th National Conference on Electrical and Electronics Engineering (ELECO)*, 2024; pp. 1–5. DOI: <https://doi.org/10.1109/ELECO64362.2024.10847078>
- [34] Wei, Z.; Chen, J.; Tang, H.; Zhang, H. (2024). RSSI-based location fingerprint method for RFID indoor positioning: A review, *Nondestructive Testing and Evaluation*, 39, 3–31, 2024. DOI: <https://doi.org/10.1080/10589759.2023.2253493>
- [35] Weiss, P. (2021). The Global Positioning System (GPS): Creating satellite beacons in space, engineers transformed daily life on earth, *Engineering*, 7, 290–303, 2021. DOI: <https://doi.org/10.1016/j.eng.2021.02.001>
- [36] Xu, Z.; Huang, B.; Jia, B.; Mao, G. (2023). Enhancing WiFi fingerprinting localization through a co-teaching approach using crowdsourced sequential RSS and IMU data, *IEEE Internet of Things Journal*, 11(2), 3550–3562, 2023. DOI: <https://doi.org/10.1109/JIOT.2023.3297521>
- [37] Yang, T.; Cabani, A.; Chafouk, H. (2021). A survey of recent indoor localization scenarios and methodologies, *Sensors*, 21, 8086, 2021. DOI: <https://doi.org/10.3390/s21238086>



Copyright ©2026 by the authors. Licensee Agora University, Oradea, Romania.

This is an open access article distributed under the terms and conditions of the Creative Commons Attribution-NonCommercial 4.0 International License.

Journal's webpage: <http://univagora.ro/jour/index.php/ijccc/>



This journal is a member of, and subscribes to the principles of,
the Committee on Publication Ethics (COPE).

<https://publicationethics.org/members/international-journal-computers-communications-and-control>

Cite this paper as:

Bandirmali Erturk, N.; Tekkol, T. Crowd-Resilient Wi-Fi Indoor Localization Framework Using Ensemble Regression Models, *International Journal of Computers Communications & Control*, 21(2), 7411, 2026.

<https://doi.org/10.15837/ijccc.2026.2.7411>